

Article

Linking Microbial Functioning and Trophic Pathways to Ecological Status in a Coastal Mediterranean Ecosystem

Franco Decembrini ¹, Carmela Caroppo ^{2,*}, Gabriella Caruso ¹ and Alessandro Bergamasco ³

¹ Institute of Polar Sciences, National Research Council (CNR-ISP), Section of Messina, Spianata S. Raineri 86, 98122 Messina, Italy; franco.decembrini@cnr.it (F.D.); gabriella.caruso@cnr.it (G.C.)

² Water Research Institute, National Research Council (CNR-IRSA), Section of Taranto, Via Roma 3, 74121 Taranto, Italy

³ Institute of Marine Sciences, National Research Council (CNR-ISMAR), Section of Venice, Castello 2737/F, 30122 Venice, Italy; alessandro.bergamasco@ismar.cnr.it

* Correspondence: carmela.caroppo@irsa.cnr.it; Tel.: +39-0994542211

Citation: Decembrini, F.; Caroppo C.; Caruso, G.; Bergamasco, A. Linking Microbial Functioning and Trophic Pathways to Ecological Status in a Coastal Mediterranean Ecosystem *Water* **2021**, *13*, 1325. <https://doi.org/10.3390/w13091325>

Academic Editor: Maria Moustaka-Gouni

Received: 30 March 2021

Accepted: 6 May 2021

Published: 10 May 2021

Publisher's Note: MDPI stays neutral with regard to jurisdictional claims in published maps and institutional affiliations.



Copyright: © 2021 by the authors. Licensee MDPI, Basel, Switzerland. This article is an open access article distributed under the terms and conditions of the Creative Commons Attribution (CC BY) license (<https://creativecommons.org/licenses/by/4.0/>).

Abstract: Coastal marine ecosystems host complex microbial communities whose composition and metabolism are influenced by continental inputs and mesoscale properties of seawater masses. The identifying traits of the phytoplankton and bacteria such as biomass, size, shape and their metabolism related to organic matter production and degradation, recognized as indicators of the functioning of an ecosystem, were observed in the Gulf of Manfredonia (South Adriatic Sea, Italy) in late spring. This Gulf area is characterized by terrestrial inputs and mesoscale circulation influence such as coastal waters flowing southward from the North Adriatic and offshore waters interested by the Ionian Sea. Water samples were grouped in clusters (Coastal, Intermediate, Offshore and Deep Systems) according to the water column properties. Phytoplankton community biomass and composition, autotrophic and total prokaryotic abundances and microbial metabolism such as enzyme activity rates and prokaryotic heterotrophic production were analyzed to elucidate the trophic pathways with the objective to infer on the ecosystem status. As expected, size-fractionated phytoplankton biomass and production showed greater concentration in coastal waters with prevalence of the largest fractions (micro- and nano-) supported by the diatoms. Conversely, lower biomass and production were measured in all off-shore waters, mainly sustained by smallest fractions (nano-sized phytoflagellates and picophytoplankton). Total and autotrophic prokaryotic abundance decreased from coastal to offshore stations, inversely with respect to cell volume. Prokaryotic heterotrophic production was just below 50% compared to that of phytoplankton in all waters, evidencing an active biomass synthesis. High alkaline phosphatase and leucine aminopeptidase in coastal and offshore waters suggested the quick regeneration of Phosphorus and protein decomposition, respectively. Different levels of phytoplankton-bacteria association might provide a tool to define the ecological status of the studied system in the observed period; an approach to ecosystem assessment exportable to other coastal systems is proposed.

Keywords: size-fractionated plankton; phytoplankton biomass; phytoplankton production; species composition; prokaryotic traits; prokaryotic production; microbial enzyme activity; Southern Adriatic Sea

1. Introduction

Microbial community structure and function play a crucial role in ecosystem dynamics, regulating at microscale level biogeochemical processes that have important implications at macroscale and global levels; thus, an accurate view of the ecosystem functioning is achieved only through a multifaceted vision of microbial community in terms of abundance, structure and metabolic activity [1]. A holistic approach to the study of all the components of an ecosystem, including the smallest size ones, is needed to obtain

a comprehensive understanding of its functioning. Phytoplankton, through the biomass and activity of its different size components (micro-, nano- and pico- fractions), triggers the main pathways of biogenic Carbon assimilated through the food web and affects the whole environmental trophic conditions [2]. Phytoplankton diversity, due to a number of very diverse organisms (prokaryotes and eukaryotes, autotrophic and mixotrophic), has a fundamental role in the functioning of ecosystems. These microorganisms, organized in complex associations, are deeply entangled in food-webs and biogeochemical cycles [3]. On the other hand, microbial communities through their hydrolytic enzymes decompose organic polymers into simpler monomers, recycling nutrients such as Phosphorus and Nitrogen that are utilized to support primary production [4,5]. Moreover, even if few studies are available [6,7] bacterial activity could be a function of bacterial size [8].

Typically, coastal marine environments are eutrophic systems with high concentrations of inorganic nutrients, sustaining high productivity; here, larger phytoplankton and phagotrophic heterotrophs prevail over prokaryotic heterotrophs. Conversely, pelagic environments are oligotrophic systems characterized by low nutrient concentrations, with high amounts of dissolved nutrients in organic form, which favor prokaryotic heterotrophs over small phytoplankton [9].

Two main trophic pathways are generally recognized, i.e., the herbivorous food web, controlled by large phytoplankters and grazing, and the microbial loop food web, controlled by smaller recycling organisms and zooflagellate grazers. In-between, a continuum trophic pathway, including the multivorous and microbial webs, has been hypothesized to exist [10,11].

The Mediterranean Sea is recognized as one of the most oligotrophic marine basins in the world, where the microbial food web is predominant [12–14]. The prevalence of both auto- and heterotrophic prokaryotes in the Mediterranean area suggests that prokaryotes are actively involved in organic matter recycling to sustain primary production process and that only a low fraction of energy is transferred to high trophic levels [13,15].

Although environmental factors (temperature and circulation of water masses) and primary productivity act as major drivers in affecting the food web dynamics [15,16], the links between the prokaryotic (auto- and heterotrophic) components and their functional roles are not well known [17].

For the first time in the South Adriatic Sea, in this study, we looked with a holistic approach at the overall functioning of the microbial compartment, in order to highlight, if any, functioning differences between coastal and pelagic systems and possible relations with mesoscale processes. Our general purpose is to define the main characteristics of the trophic pathways of the planktonic compartment in the sub-systems of the Gulf of Manfredonia. In particular, we aim at describing the size structure (as pico-, nano- and micro-fractions) in terms of biomass and diversity of the prokaryotic and eukaryotic communities as well as their role in organic matter synthesis and decomposition processes. The specific objective is to test, in a well-defined late spring case-condition, whether microbial parameters can be suitable environmental descriptors and used to assess the ecological quality of this ecosystem. The ultimate scope of our research is to provide a solid baseline for a broader application to other coastal ecosystems.

2. Materials and Methods

2.1. Study Area

The Gulf of Manfredonia, located in the South-East of the Gargano promontory (South Adriatic Sea), is an area subject to agricultural, industrial and urban impacts [18], still little investigated from a biogeochemical point of view [19–21]. Morphologically, the Gulf of Manfredonia has high and rocky coasts in the north and in its central and south area, up to Barletta. The Western Adriatic Current (WAC) flows southward offshore the Gargano promontory, generating an anticyclonic circulation within the central area of the

Gulf that results in water masses mixing (Figure 1). The predominant winds blow from N-NW and secondly from S-SE, generating surface currents with cyclonic or anticyclonic circulation, respectively. The Gulf receives the outflows from the Ofanto and some minor rivers (Carapelle, Candelaro and Cervaro). Ofanto river represents an important source of sedimentary material contributing to the main continental inputs into the Gulf [22]. Alongshore transport is usually towards SE, due to geostrophic coastal currents from the North Adriatic and is affected by the dominant cyclonic water mass circulation in the Adriatic. The platform has a slightly marked bathymetric profile.

2.2. Sampling

The sampling cruise (SAMCA Project) was conducted on board of the R/V Urania (from 15th to 26th May 2003) at fifteen hydrographic stations located on four coastal-offshore transects laying in the Gulf of Manfredonia (41° N– 15.5° E and 42° N– 17.5° E, Figure 1). The sampling design was conceived to link microbial functioning and trophic pathways to mesoscale processes and it included eight stations (stations 24,25, 32,33, 39–42) in the main middle transect crossing the Gulf from 15 to 250 m of depth, four stations (stations 4, 7, 43, 44) at the northern entrance, to intercept the lateral inputs brought by the Western Adriatic Current (WAC) and three stations (stations 35, 36, 38) at the southern border, to detect the characteristics of the waters leaving the Gulf. More information on the sampling stations is reported in Table S1.

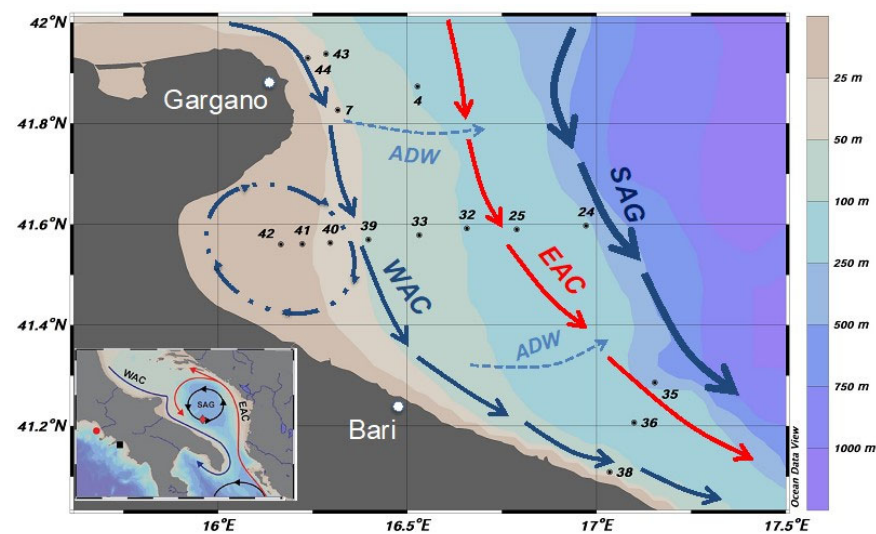


Figure 1. Location of sampling stations in the Gulf of Manfredonia (South Adriatic Sea). The continuous arrows show the paths of the main currents: the Adriatic Surface Water (ASW) characterized by relatively low salinity due to riverine inputs flows geostrophically South-Eastward along the Italian coast and is called Western Adriatic Current (WAC); in the lee side of the Gargano promontory, a slow anticyclonic recirculation cell is induced in the Gulf. The Adriatic Deep Water (ADW, indicated by dashed arrows) forms in winter due to open convection mechanisms and spills deeper through the shelf canyons. Ionian Surface Water (ISW) enters the basin along the Albanian coast as Eastern Adriatic Current (EAC) and form the South Adriatic Gyre (SAG) [23–27].

2.3. Physical-Chemical Parameters

Vertical profiles of temperature (T) and salinity (S) were recorded by a SeaBird 911plus CTD-O-FI profiler equipped with a Scufa (Turner) fluorometer; CTD was armed with a Rosette sampler hosting 24×10 L Niskin bottles.

Chemical analyses for nutrients (ammonia, nitrite, nitrate, orthophosphate concentrations) were performed according to conventional laboratory methods [28,29].

2.4. Total and Size-Fractionated Chlorophyll *a* and Primary Production Rates

Chlorophyll *a* (chl*a*) and phaeopigments (phaeo) concentrations were measured by fluorometry. Samples (1.5–2.0 L) were sequentially filtered after collection on polycarbonate (10.0 and 2.0 μm) and on Whatman GF/F filters to separate three size classes of autotrophic plankton: micro- (> 10.0 μm) nano- (10.0–2.0 μm) and pico-phytoplankton (2.0–0.2 μm). Filters were stored at $-20\text{ }^{\circ}\text{C}$ until the laboratory analysis. The chl*a* and phaeo were extracted in a 90% acetone solution, for 24 h in the dark at $4\text{ }^{\circ}\text{C}$, and measured with a Varian (mod. Cary Eclipse) spectrofluorometer before and after acidification with hydrochloric acid (0.001 N final concentration). Three readings per sample were performed, each with an integration time of three seconds. Excitation and emission wavelengths (429 and 669 nm) were selected after standardization with a solution of chl*a* extracted from *Anacystis nidulans* (by Sigma Co, Milan, Italy) [30]. The chl*a* and phaeo concentrations were calculated according to Lorenzen [31] and can be used as proxy of phytoplankton biomass, e.g., [32].

Primary production (PP) of the three size classes (as reported for the chl*a*) was measured with the standard ^{14}C label technique [33]. Samples were incubated in an “on-deck” continuous-seawater-flow incubator equipped with a set of neutral density screens, in order to reproduce the irradiance intensities (PAR % E_0) at the sampling depth. After four hours of light exposure, samples were filtered as described for chl*a*. Filters were transferred into 20-mL vials with 10 mL of “Aquasol2” scintillation cocktail and radioactivity was assessed in a liquid scintillation counter (Beckman LS1801). Readings of samples were performed until the statistical significance of dpm (disintegration per minute) was reached [34]. Alkalinity and pH were measured on board using the potentiometric method and the available total carbon dioxide calculated by Strickland and Parsons’s [29] tables.

2.5. Prokaryotic Abundance and Morphotypes

In order to estimate the picoplankton abundance, water samples were preserved with formaldehyde (2%) and kept at $4\text{ }^{\circ}\text{C}$ until they could be counted (within four weeks). The cell counts were made using a Zeiss Standard Axioplan epifluorescence microscope equipped with a halogen (Hg 100) lamp.

For pico-phytoplankton (or autotrophic picoplankton) abundance (PPA) determination, duplicate slides were prepared from each sample by filtering 10 mL of seawater through 0.2 μm (pore size) Millipore black membranes. Under blue light excitation, cyanobacterial cells fluoresced yellow-orange whereas eukaryotic algae fluoresced deep red. A BP 485/20 exciter filter, a FT 510 chromatic beam splitter and a LP 520 barrier filter were used.

For total picoplankton (PPT) duplicate slides were prepared from each sample by filtering 1 mL of seawater through a 0.2 μm (pore size) Millipore filter and staining with DAPI (4,6-diamidino-2 phenyl-indole) as fluorochrome [35]. A G 365 exciter filter, a FT 395 chromatic beam splitter and a LP 420 barrier filter were used. At least 40 microscopic fields at 1000 \times magnification were counted per each preparation. The abundance of the heterotrophic picoplankton was obtained by the difference PPT- PPA.

Cell size of PPA and PPT was estimated by epifluorescence microscopy using microphotographs. Each cell size was determined after projection on a screen; over at least 60 cells per filter were measured manually. For PPA, cell volume was calculated assuming that the shape of picoplankton was spherical or cylindrical with hemispheric ends [36] and using the Bratbak’s [37] formulas. PPT cells were subdivided into eight size classes: three size classes of cocci (0.065, 0.321 and 0.523 μm^3) and five size classes of rods (0.196, 0.294, 0.393, 0.491 and 0.589 μm^3).

2.6. Larger Phytoplankton Abundance and Species Composition

Water samples destined to phytoplankton analysis were collected in 500 mL dark glass bottles, preserved with an acid Lugol's iodine solution to a final dilution of 1.0% and stored at 4 °C until analysis. Identification and counting were performed by using an inverted microscope (Labovert FS Leitz) equipped with phase contrast and following the Utermöhl method [38]. With the term "larger phytoplankton", we considered the so called "Utermöhl phytoplankton", which includes all nano- and micro- phytoplankton taxa recognizable in light microscopy. Nano-phytoplankton (2–20 µm) was analyzed at a magnification of 630× in random fields until at least 100 cells of the most abundant group were counted. Regarding the phytoflagellates, a distinction between photosynthetic and non-photosynthetic species was made using the information available in the literature, e.g., [39]. Micro-phytoplankton (20–200 µm) counts were performed along transects (1–4) or in random fields (30–60); in addition, half of the Utermöhl chamber was also examined at a magnification of 200×, to obtain a more correct evaluation of less abundant taxa.

2.7. Extracellular Enzyme Activity Rates (EEA)

Total extracellular enzymatic activity (EEA) rates were immediately measured after sample collection, using fluorogenic substrates [the methylumbelliferyl (MUF)-derived compounds MUF-phosphate and MUF-β-Glucopyranoside (Sigma-Aldrich Corporate, Merck Life Science, Milan, Italy) for alkaline phosphatase (AP) and β-glucosidase (GLU) activities, respectively, and the methylcoumarine (MCA)-derived compound L-leucine-7-amido-4-methylcoumarin hydrochloride (Sigma-Aldrich) for leucine aminopeptidase (LAP) activity, according to a multi-concentration method [40]. Five increasing concentrations of each fluorogenic substrate (from 0.1 to 20 µM) were added to triplicate 10 mL water samples; sterile prefiltered seawater was used as the blank. Incubation was carried out at in situ temperature for 3 h. The fluorescence released by substrate hydrolysis was measured with a Turner TD 700 fluorometer, equipped with 380–440 and 365–445 nm filters (excitation-emission wavelengths) for Leu-MCA and MUF substrates, respectively. The increase of fluorescence was converted into the hydrolysis velocity using a standard curve of MUF and MCA [41,42].

2.8. Prokaryotic Heterotrophic Production (PHP)

PHP was estimated from the rate of [³H] leucine incorporation using the micro centrifugation method according to Smith and Azam [43], incubating in the dark, for 1.5 hr at in situ temperature, triplicate samples and two blanks with L-[4,5 ³H] leucine (Amersham Biosciences Limited, Little Chalfont, UK) (25 nM final concentration). The incorporation of tritiated leucine was stopped by the addition of 90 µL of TCA 100%; after a rinse with ethanol 80%, PHP was calculated according to Kirchman [44] using in situ determination of leucine Isotopic Dilutions (ID) performed using a kinetic approach [45]. The ID of the leucine added from other sources of natural leucine (X-axis intercept, expressed in nM) was calculated by plotting the reciprocal of the labeled leucine uptake (LU) rate (in dpm of labelled leucine L⁻¹ h⁻¹) versus the concentration of added total leucine (in nM) [42]. The calculation of the ID was adjusted to 20 nM leucine, which was the concentration of leucine used in the routine assays. In the ID assay, the optimal ³H-leucine concentration and time of incubation were also determined.

2.9. Data Processing and Statistical Analysis of Dataset

The abbreviations of the studied parameters are listed in Table S2.

CTD data were processed with Ocean Data View (ODV) software [46] to obtain T/S diagram. The agglomeration distance plot of salinity values at different depths guided the formation of four clusters from the 131 pairs of available observations. To ensure a good ability of separation in case of noise between clusters, Ward's hierarchical clustering with Manhattan distance method was adopted [47]. To test the strength of the pre-defined

grouping, a multivariate analysis (Canonical Variates Analysis, CVA) [48] was carried out on the environmental data (results are shown Figure S1a).

To test for significant differences between and within groups of data, one-way ANOVA and parametric (Fisher's LSD on means) or non-parametric (Kruskal–Wallis on medians, in case of non-homogeneity of variances) tests were used.

For phytoplankton, the significance of spatial differences in community composition between water masses (the three salinity vs. depth clusters, excluding the deep one) was tested using a one-way Analysis of Similarities (ANOSIM) routine in PRIMER [49]. Bi-dimensional representations of the statistical comparisons among water masses and stations were obtained by non-parametric multidimensional scaling (nMDS) and cluster analysis performed on Bray–Curtis similarity matrices (fourth root-transformed data) [49]. The choice of best level of transformation derives from the visualization of the Shade Plots (PRIMER procedure), which are simple visual representations of the abundance matrix. These plots represent an effective aid in choosing an overall transformation of quantitative data, striking an appropriate balance between dominant and less abundant taxa in ensuing resemblance-based multivariate analyses [50]. For each nMDS plot, stress values were shown to indicate the strength of representation of differences among samples [51]. The nanoplankton categories, very abundant at all stations, were excluded from the data matrix, in order to enhance the role of the less abundant and rare species in determining similarity among samples.

A one-way similarity percentage procedure (PRIMER SIMPER routine) was used to obtain the percentage contribution of each category to the Bray–Curtis similarity between the groups of samples in the three clusters.

To evaluate the relationships between microbial and physical-chemical parameters, a CCA (Canonical Correlation Analysis) [52,53] was firstly performed (see Figure S1b) then Pearson's correlations were used to discuss relevant pairwise relations.

3. Results

3.1. Physical-Chemical Variables

T/S diagram in Figure 2a clearly distinguished coastal stations (<50 m) influenced by the less salty Western Adriatic Current with respect to offshore stations (>50 m isobaths) featuring salinity above the threshold value of 38.6 and influenced by the South Adriatic Gyre that carries mixed waters of Ionian origin.

Using salinity itself and depth as key drivers, cluster analysis on samples identifies four systems: Coastal (CS), Offshore (OS), Intermediate (IS) and Deep (DS) (Table 1, Tables S3, S4 and S6). This latter System includes only few samples due to the bathymetric constraints and is considered only as a reference for the others.

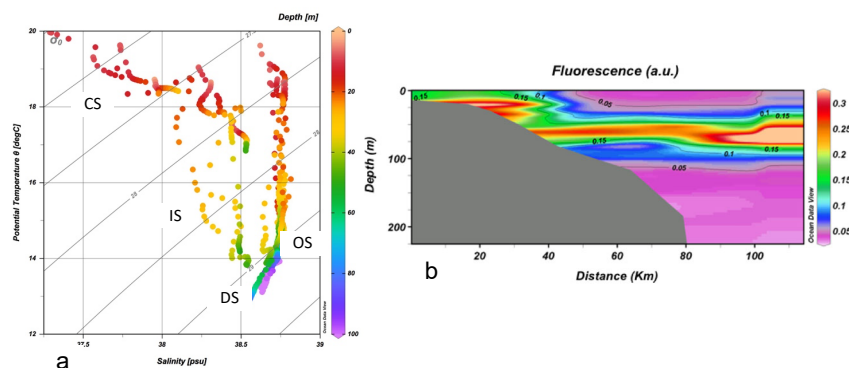


Figure 2. (a) Temperature (°C)/Salinity (T/S) diagram of CTD measurements and samples bounding in assigned clusters (Coastal (CS), Offshore (OS), Intermediate (IS) and the Deep (DS) Systems) according to the salinity and depth; (b) vertical section of fluorescence from chl a along the central transect in the Gulf area.

Table 1. Average values and standard deviations of the main water and biotic parameters measured in the identified Clusters: Coastal (CS), Intermediate (IS), Offshore (OS) and Deep (DS) Systems in the Gulf area.

Parameter	Fraction/Species	Unit	System											
			CS			IS			OS			DS		
			Avg	SD	n	Avg	SD	n	Avg	SD	n	Avg	SD	n
T		°C	18.60	0.86	15	15.46	2.06	22	15.87	2.09	24	13.73	0.26	3
S		psu	37.89	0.24	15	38.50	0.14	22	38.73	0.04	24	38.69	0.05	3
δt		kg m ⁻³	27.33	0.38	15	28.55	0.56	22	28.64	0.51	24	29.10	0.02	3
O₂		mL L ⁻¹	5.66	0.19	15	6.01	0.28	22	5.87	0.29	24	5.65	0.19	3
PO₄			0.06	0.03	13	0.06	0.04	12	0.09	0.04	17	0.12	0.04	2
NH₄			0.41	0.21	14	0.44	0.37	14	0.54	0.37	19	1.07	0.47	2
NO₃		μM	0.55	0.21	14	0.63	0.39	11	0.84	0.39	16	1.42	0.45	2
NO₂			0.10	0.05	13	0.10	0.08	14	0.07	0.06	15	0.06	0.02	2
Si(OH)₄			1.37	0.27	6	1.16	0.56	4	0.75	0.57	10			
chl_a	Tot.		0.51	0.29	13	0.21	0.13	13	0.10	0.09	20			
	> 10 μm	μg L ⁻¹	0.29	0.21	13	0.08	0.09	11	0.03	0.03	15			
	10-2 μm		0.13	0.08	13	0.04	0.02	11	0.01	0.01	15			
	2-0.5 μm		0.09	0.04	13	0.09	0.04	11	0.04	0.03	15			
phaeo	Tot.		0.12	0.08	13	0.07	0.03	13	0.09	0.07	19			
	> 10 μm	μg L ⁻¹	0.06	0.06	13	0.02	0.01	11	0.03	0.03	15			
	10-2 μm		0.03	0.02	13	0.01	0.01	11	0.01	0.01	15			
	2-0.5 μm		0.03	0.01	13	0.03	0.01	11	0.03	0.02	15			
PP	Tot.		2.39	2.03	9	1.84	1.19	8	0.82	0.36	10			
	> 10 μm	μgC L ⁻¹ h ⁻¹	1.19	1.04	9	0.57	0.38	8	0.30	0.25	10			
	10-2 μm		0.71	0.65	9	0.25	0.16	8	0.10	0.08	10			
	2-0.5 μm		0.49	0.69	9	1.01	0.99	8	0.42	0.20	10			
PHP		μgC L ⁻¹ h ⁻¹	0.31	0.15	15	0.09	0.08	21	0.04	0.03	20	0.03	0.04	3
AP			41.95	12.88	15	26.64	20.05	21	35.72	43.86	24	61.53	105.89	3
LAP		nM h ⁻¹	14.21	9.04	14	20.42	21.95	21	23.40	19.77	24	6.43	5.96	3
a-Glu			0.94	0.63	15	0.48	0.53	20	0.59	0.63	23	0.190	0.157	3
b-Glu			1.17	0.78	15	0.49	0.57	18	0.40	0.40	24	0.244	0.243	2
PPA		cells x 10 ⁶ L ⁻¹	7.08	3.51	16	5.47	3.15	22	4.78	4.11	24	1.30	1.05	3
PPT		cells x 10 ⁸ L ⁻¹	1.94	1.15	16	1.24	0.62	22	1.02	0.41	24	1.13	0.15	3
PPT	Cocci 0.5 μm		0.69	0.35	15	0.46	0.24	19	0.36	0.14	24	0.18	0.15	3
	Cocci 0.85 μm		0.20	0.22	15	0.15	0.11	19	0.10	0.09	24	0.02	0.03	3
	Cocci 1.0 μm		0.00	0.00	15	0.01	0.02	19	0.01	0.01	24	0.16	0.15	3
	Rods 1.0 μm	cells x 10 ⁸ L ⁻¹	0.70	0.42	15	0.51	0.24	19	0.40	0.17	24	0.26	0.20	3
	Rods 1.5 μm		0.22	0.22	15	0.14	0.14	19	0.12	0.07	24	0.04	0.05	3
	Rods 2.0 μm		0.04	0.09	15	0.03	0.05	19	0.03	0.03	24	0.01	0.01	3
	Rods 2.5 μm		0.01	0.03	15	0.00	0.01	19	0.01	0.01	24	0.00	0.00	3
	Rods 3.0 μm		0.00	0.00	15	0.00	0.00	19	0.00	0.01	24	0.80	0.70	3
Phytoplankton	Total		7.81	2.28	16	5.28	2.05	22	6.69	2.63	24	2.14	0.50	3
	Diatoms		3.99	2.37	16	1.71	1.17	22	3.06	2.20	24	0.49	0.11	3
	Dinoflagellates	cells x 10 ⁴ L ⁻¹	0.79	0.42	16	0.48	0.32	22	0.73	0.44	24	0.15	0.10	3
	Coccolithoph.		0.15	0.18	16	0.16	0.16	22	0.19	0.15	24	0.10	0.08	3
	Other Phytoflag.		2.88	0.70	16	2.93	1.25	22	2.71	1.20	24	1.41	0.37	3

Nutrient concentrations are generally low and homogenous throughout the Gulf (Table S3), with a weak increase from OS to CS, though relevant production processes induce here high nutrient uptake, especially of phosphate and silicate, in particular by diatoms. Nitrate and ammonium, although at low concentrations, do not appear to limit phytoplankton growth and show significant ($p < 0.05$) differences among the Systems, with minimum values in CS.

3.2. Distribution of Size-Fractionated Chlorophyll a and Phaeo-Pigments

Phytoplankton biomass expressed in terms of *chl a* concentration ranges between $0.03 \mu\text{g L}^{-1}$ (in OS) and $1.3 \mu\text{g L}^{-1}$ (in CS) with an overall mean of $0.25 \pm 0.24 \mu\text{g L}^{-1}$ and a ratio *chl a* vs. degraded pigments (phaeo) of 67%. The vertical distribution patterns across the Gulf (from in situ fluorescence, Figure 2b) highlight a core with highest values at surface in CS while a Deep Chlorophyll Maximum (DCM) is observed in OS in the 50–75 m layer. Total *chl a* concentration shows a clear decreasing gradient towards the open sea with significantly higher values in CS than elsewhere ($p < 0.05$) and a more active community in CS (ratio *chl a* vs. phaeo pigments of 81%) compared to the other Systems (IS = 71% and OS = 53%). Size incidence shows that the micro-fraction prevails mainly in CS (57%), while it is matched in IS (41%) by the pico-fraction that slightly prevails in OS (42%). ANOVA confirms that micro- and nano- sized *chl a* fractions dominate significantly ($p < 0.05$) in CS whereas the pico-sized fraction is significantly ($p < 0.05$) different in OS with respect to the other Systems. Total and pico-sized degraded pigments are quite homogeneously distributed throughout the area, while micro- and nano-sized phaeo are significantly higher in CS than in IS ($p < 0.05$) and OS ($p < 0.05$), respectively.

3.3. Indices of Phytoplankton Functionality

Total Primary Production shows an average rate of $1.6 \pm 1.5 \mu\text{gC L}^{-1} \text{h}^{-1}$ ($0.4\text{--}6.5 \mu\text{gC L}^{-1} \text{h}^{-1}$) sustained by micro- and nano-fractions (40% each) and tracks the *chl a* distribution, with values decreasing from CS to OS and a wider data dispersion mainly in CS. However, no significant differences among the three Systems are found ($p > 0.05$). Size contribution indicates that the micro- fraction significantly dominates (Kruskal–Wallis, test on medians, $p < 0.03$) in CS (46%) at the highest PP rates, while the pico-fraction is the most active component in IS (48%) and OS (52%), although not significantly.

The PP/*chl a* ratio (Assimilation Number, AN, [54]) expresses the Carbon assimilation capacity of phytoplankton per biomass unit; it is generally low in CS (average $6 \mu\text{gC h}^{-1}/\mu\text{g-chl a}$), while doubles in OS both for micro- and pico- fractions (5.7 to $13.8 \mu\text{gC h}^{-1}/\mu\text{g-chl a}$ and 7.1 to $13.4 \mu\text{gC h}^{-1}/\mu\text{g-chl a}$, respectively) while the nano-fraction AN is almost constant in all the Systems (CS = 7.5; IS = 8.3 and OS = 7.8 $\mu\text{gC h}^{-1}/\mu\text{g-chl a}$) (Figure 3).

Despite their wide variability, the AN values do not show significant differences in both the total and fractionated phytoplankton among the Systems ($p > 0.05$).

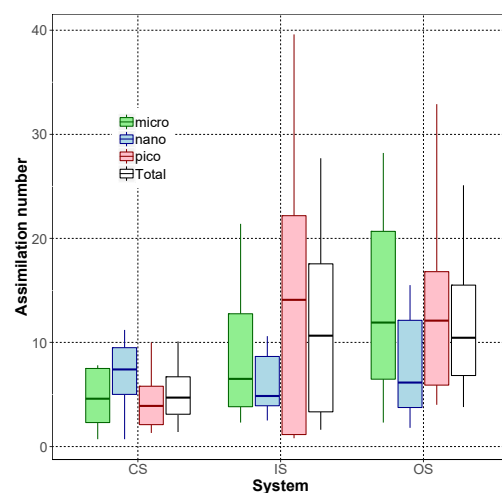


Figure 3. Boxplots of the Assimilation Number (AN, $\mu\text{gC h}^{-1}/\mu\text{g-chl a}$) of total and size-fractionated (micro-, nano- and pico) phytoplankton in the Coastal (CS), Offshore (OS) and Intermediate (IS) in the Gulf area.

3.4. Structure of the Prokaryotic Community

PPA values are on average $5.4 \pm 3.8 \times 10^6$ cells L⁻¹, while PPT shows a mean value of $1.3 \pm 0.8 \times 10^8$ cells L⁻¹. Spatial distribution of PPA and PPT depicts decreasing patterns from CS to OS (Tables 1 and S4, Figure 4). ANOVA reveals that PPA is significantly higher in CS than in DS as expected ($p = 0.05$) but similar between IS and OS.

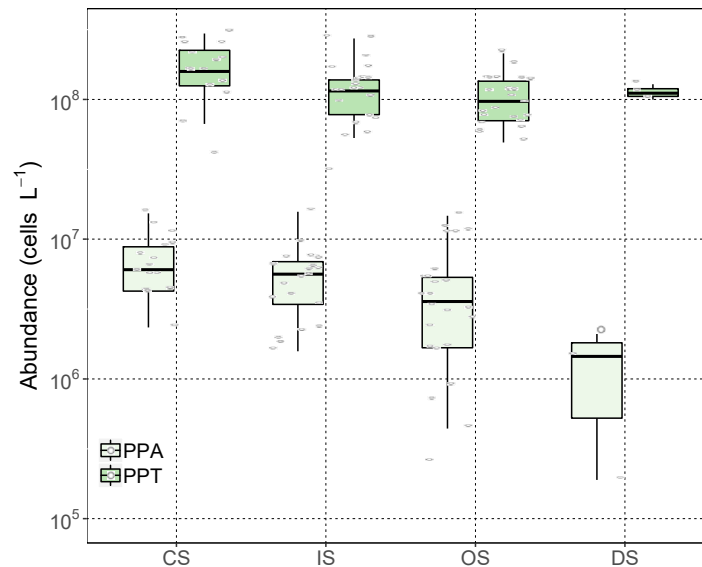


Figure 4. Boxplots of autotrophic (PPA) and total (PPT) prokaryotic community in the Coastal (CS), Offshore (OS), Intermediate (IS) and Deep (DS) Systems in the Gulf area.

PPT is significantly higher in CS compared to IS and OS (Mood's median test $p < 0.05$). From a qualitative point of view, PPT is mainly represented by the smallest components of the community: cocci (0.5 μm , accounting for 35.0%; 0.85 μm , 10.5% of the total abundances) and rods (1.0 μm , 38.9%; 1.5 μm , 11.8%). Differences are found as for the total cocci (Fisher LSD test, $p < 0.05$) and total rods ($p < 0.05$), which are both significantly higher in CS than in the others mainly depending on the smallest components of the prokaryotic community: cocci 0.5 μm (multirange test, Fisher LSD, $p < 0.05$) and rods 1.0 μm ($p < 0.05$).

3.5. Structure of the Large Phytoplankton Communities

Phytoplankton abundances range between 1.5 and 14.0×10^4 cells L⁻¹, with average values of $6.2 \pm 2.5 \times 10^4$ cells L⁻¹. The highest concentrations are detected in the CS (Figure 5a, Table 1, Table S4) and significant differences emerge between CS and IS ($p < 0.05$) and between OS and IS ($p < 0.05$). Such differences are due to diatoms and dinoflagellates, which have higher concentrations in CS than in IS ($p < 0.05$) while coccolithophorids ($p = 0.78$) and "other phytoflagellates" ($p = 0.16$) are uniformly distributed throughout the Systems.

The phytoplankton community is dominated by "other phytoflagellates" that represent on average about the $47.6 \pm 16.3\%$ of the total abundance. They mainly included small forms (<10 μm) of uncertain taxonomic identification (97.8%); chloro-, eugleno-, prasino- and dictyochophyceae account only for 2.2%. Diatoms and dinoflagellates average $39.6 \pm 17.4\%$ and $10.2 \pm 6.0\%$, respectively. In general, coccolithophorid abundances are scarce, corresponding on average to $2.6 \pm 2.4\%$ with the nano-sized *Emiliania huxleyi* as dominant species (95.5%).

A total of 100 taxa including 54 diatoms, 42 dinoflagellates and 2 coccolithophores were identified considering also 2 species classified in the group “other phytoflagellates” (Table S5).

In the Gulf area, the phytoplankton community is represented by many species and dominance phenomena are not detected by the Rank Abundance Distributions (RADs data not shown).

Only four species account for more than 15% of the total abundances and are differently spread across the Systems (Figure 5b). *Cylindrotheca closterium* and *Chaetoceros* spp. are mainly observed in CS and OS, respectively, whereas *Emiliana huxleyi* shows a wide distribution within the Systems with high percentages in IS. The relative contribution of *Cerataulina pelagica* is negligible with respect to the three other species.

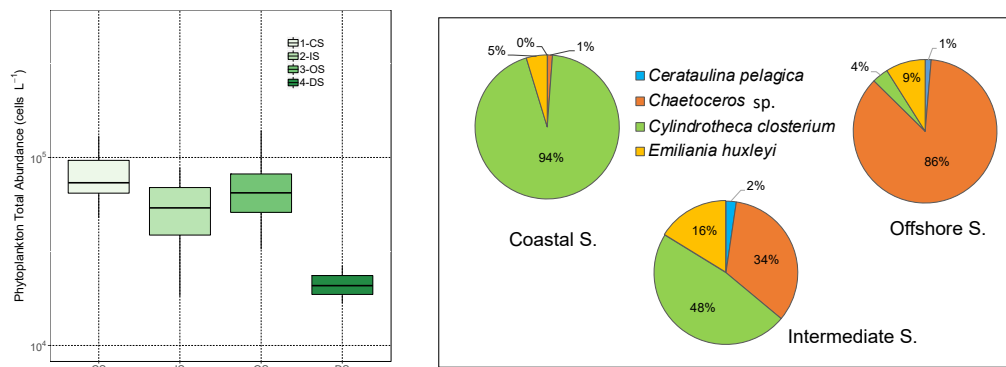


Figure 5. (a) Boxplot of total phytoplankton in the Coastal (CS), Intermediate (IS), Offshore (OS) and Deep (DS) Systems in the Gulf area; (b) Relative percentages of the four most abundant phytoplankton species (>15%) in the three Systems in the Gulf area.

As concerns the phytoplankton species distribution, a significant partitioning in all the Systems has been found (ANOSIM, $R = 0.381$, $p = 0.1\%$) confirmed by the non-overlapping between CS and OS assemblages in nMDS plot (useful stress value) (Figure 6). The average similarity in each System decreases from CS (49.1%) to OS (41.8%) and IS (34.6%) while a high average pairwise dissimilarity between the Systems is detected (OS & IS = 65.9%; OS and CS = 70.8%, IS and CS = 65.2%).

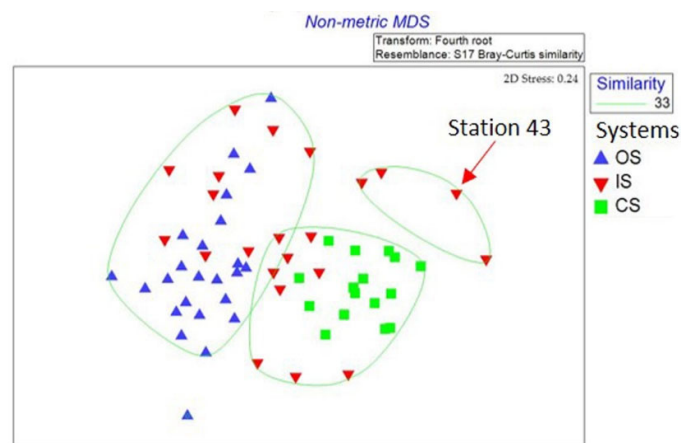


Figure 6. Non-metric multidimensional scaling (nMDS) ordination plot of the phytoplankton species abundances collected in the Coastal (CS), Intermediate (OS) and Offshore (OS) Systems. The groups identified by the green line are obtained by overlaying the cluster analysis performed on the same matrix at similarity level of 33%. Note that the station 43 (four red triangles: 0, 25, 35 and 45 m) identifies the inflow waters from the Northern Adriatic Sea.

In CS, the community is represented mainly by micro-sized species: 98% of the diatoms and 63% of the dinoflagellates. The most representative species are the diatoms *Cylindrotheca closterium*, *Pleurosigma* sp., *Navicula* sp. *Nitzschia longissima*, and the dinoflagellate *Gyrodinium fusiforme*. In IS, the micro-sized organisms are always dominant (73% of the diatoms and 59% of the dinoflagellates), even if with percentage values lower than those registered in CS. Among the species, besides the micro-sized diatom *Cerataulina pelagica*, the nano-sized *Emiliana huxleyi* is important, too. The nano-sized phytoplankton dominates in OS: 67% of the diatoms and 48% of the dinoflagellates. The most abundant species are *Chaetoceros* spp. (diatoms) and Gymnodiniales (dinoflagellates).

3.6. Microbial Activity Rates

Microbial enzyme activity rates follow the order AP > LAP > b-GLU > a-GLU.

Except for LAP, clear decreasing gradients from CS to OS and DS are found for all the metabolic activities (Tables 1 and S6). AP rates decrease from CS to IS and OS, and at DS the minimum AP is found, apart for station 35-257 m, where this enzyme reaches its maximum activity (in correspondence with a high PPA), resulting in high variability. A similar decreasing trend from CS towards OS is depicted by both a- and b-GLU. More variable spatial distribution patterns are observed for LAP, which reaches its highest rate in OS, decreases in CS and IS and shows its minimum value in DS (Table S6).

No statistically significant differences in the enzyme hydrolysis rates among the Systems are detected, except for b-GLU, whose mean activity rates are significantly ($p < 0.05$) higher in CS than in OS (Kruskal–Wallis test $p < 0.05$; Mood's median test $p < 0.05$).

PHP rates range from 0.0053 to 0.579 $\mu\text{gC L}^{-1}\text{h}^{-1}$ (measured at station 24–180 m and station 42–0 m, respectively), with a mean value of $0.125 \pm 0.140 \mu\text{gC L}^{-1}\text{h}^{-1}$. PHP rates are significantly ($p < 0.05$) higher in CS than in IS and OS (not homogeneous variances, Mood's test on medians).

4. Discussion

To assess the microbial functional role in the Gulf of Manfredonia in the late spring period, as a model of other temperate marine ecosystems, the simplified scheme applied in Figure 7 includes standing stocks and processes that link autotrophic and heterotrophic compartments in a coastal system (CS) subject to terrigenous inputs and connected to a oligotrophic pelagic one (OS) influenced by meso-scale circulation.

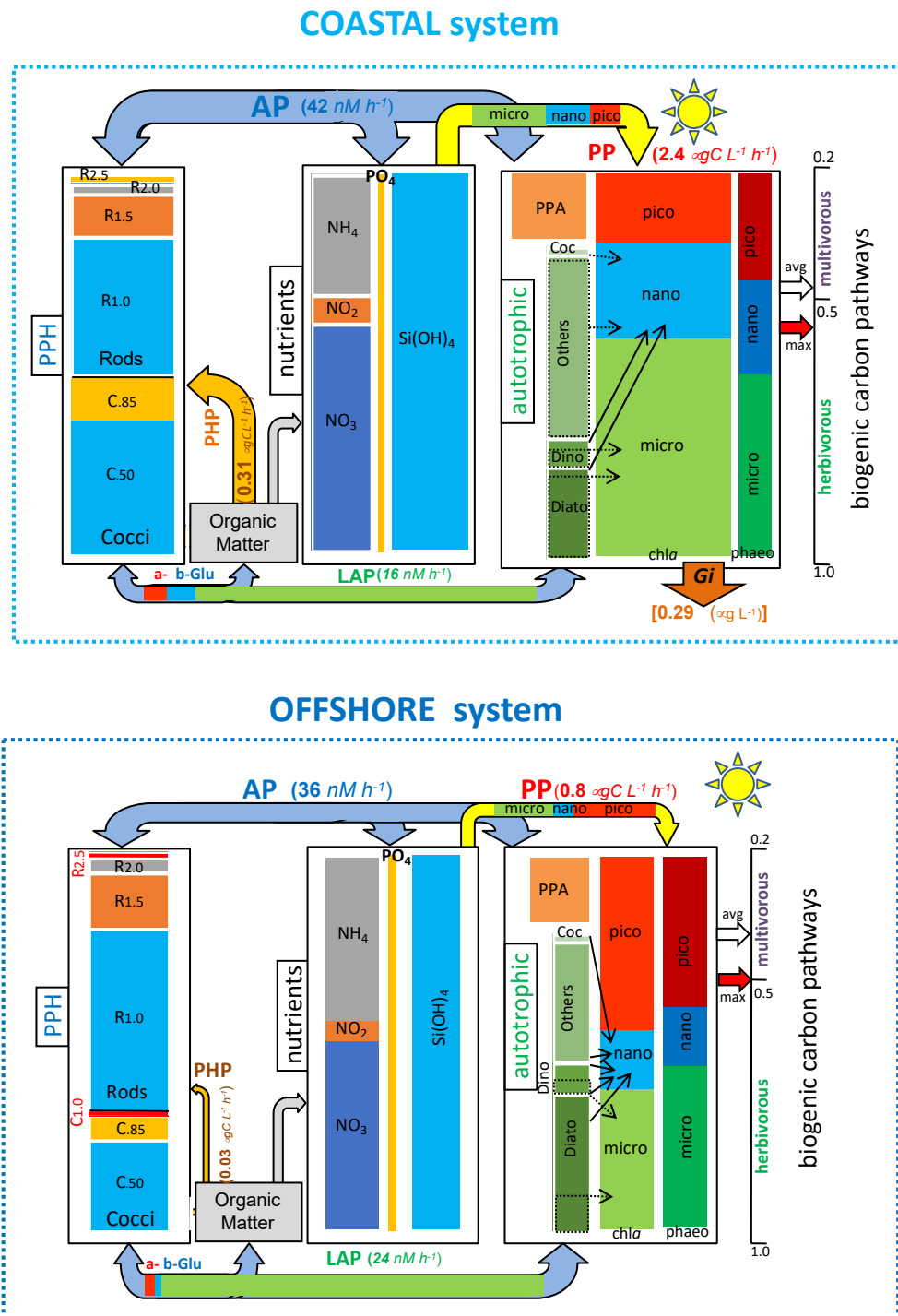


Figure 7. Simplified model of the standing stocks and metabolic processes (production and decomposition) mediated by microbial assemblages in the Coastal and Offshore Systems in the Gulf of Manfredonia in late spring period. The model shows the pools, in terms of relative concentration or abundance, of nutrients (P, DIN, Si) and autotrophic (size-fractionated *chl a* and *phaeo*, PPA and large phytoplankton main groups) and heterotrophic PPH (size-fractionated morphotypes as cocci and rods) compartments. Arrows indicate: (1) the Carbon fluxes through the autotrophic size-fractionated primary production (PP, in yellow) and the prokaryotic heterotrophic production (PHP, in orange); (2) Carbon and Phosphorus fluxes mobilized by microbes through enzymatic activities (a-Glu in red, b-Glu in blue, AP in light blue and LAP in green). Histogram/arrow widths are proportional to the total magnitude of each pool/flux. The grazing index ($G_i = \text{phaeo}/(\text{phaeo} + \text{chl a})$) [34,55] as the *chl a* potentially exported from the System is shown in dark orange. Red/White rightward arrows

indicate the biogenic-C fate in the *continuum* trophic pathway. Overall, the multivorous pathway prevails, even if the maximum value of CS points towards the herbivorous pathway. The Organic Matter (dissolved and particulate) pool (in grey) as well as the role of the eukaryotic organisms or predators of higher trophic levels in the decomposition/remineralization processes were not estimated.

4.1. Structure of Microbial Community

During late spring, in the area of the Gulf of Manfredonia, the two systems (CS and OS) are characterized by different standing stocks and trophic conditions ranging from mesotrophy (CS) to oligotrophy (OS). The autotrophic standing stocks are significantly larger in CS than OS, though sustained by a similarly large pool of residual nutrients. Picophytoplankton abundances are lower than those detected in Northern Adriatic Sea [56] and in open Southern Adriatic Sea [57] but similar to those detected in the Northern Ionian Sea [58,59] and other coastal sites ([60] and references herein). This reflects a clear influence of the Ionian waters at least in the euphotic layer of the Gulf area.

Phytoplankton biomass values, expressed as size-fractions of *chl a* and phaeopigments, confirm the above described meso-trophic scenario in CS, dominated by a slow water recirculation in the shallow shelf [26] and the oligotrophic character of OS, influenced by the South Adriatic Gyre. Scarce information on size composition of phytoplankton biomass in the Southern Adriatic Sea is available, though higher total *chl a* concentrations in spring and autumn and lower values in the other seasons were observed [56,57,61] with respect to those reported in this study.

As concerns larger phytoplankton abundances, they are lower than those previously reported in the Northern [62] and Central Adriatic Sea in the same period [63] but in the range of those observed in Southern Adriatic Sea [64–67] and the Ionian Sea [68,69].

Phytoplankton shows the presence of different associations in each of the Systems. Within CS, a well-structured community is dominated by micro-sized neritic species, such as the diatoms *Cylindrotheca closterium*, *Pleurosigma* sp., *Navicula* sp. and *Nitzschia longissima*, and different species of dinoflagellates. These taxa, with relatively low growth rates, are typical of a community moving toward a mature stage of succession (*sensu* Margalef [70]) and are well adapted to a lower water mixing of the inner stations of the Gulf. The PPA are also abundant and confirm to be an important component of the phytoplankton communities in strictly coastal sites ([60] and references herein) as well as of the entire prokaryotic community [71]. Conversely, a community typical of the first stage of the succession *sensu* Margalef [70] is observed in OS: nano-sized *Chaetoceros* and other r-strategy species dominate with the small (<20 μm) fraction of dinoflagellates (Gymnodiniales).

Trapped in-between these two Systems, cluster analysis has highlighted an intermediate condition (IS) probably influenced by the surface flow of waters originating from the North Adriatic Sea (Western Adriatic Current). Here the phytoplankton biomass, located mainly at DCM, has a double average concentration than in OS and almost one third lower than CS. IS is characterized by higher percentage of PPA, which replaces the micro-fraction observed in CS. Interestingly, the abundance of nanoplankters is constant, reflecting their ability to adapt to different environmental conditions. This is confirmed by microscopical observations, as phytoflagellates <10 μm as well as nano-sized coccolithophorids have comparable concentrations among the Systems. Moreover, larger phytoplankton community shows in IS common features with the other Systems (CS and OS), with the presence of species typical of the spring period in Adriatic Sea [57,64,67].

In addition, in CS, the abundance of total picoplankton is significantly higher than in IS and OS. Our PPT counts are comparable with those recorded in Adriatic Sea [6,7], Ionian Sea [59] and other Mediterranean systems [72].

The simultaneous occurrence of different bacterial morphotypes in marine environments has already been documented, with small sized bacteria usually inhabiting low nutrient waters [6,73]. In the study area, the smaller cocci (0.5 μm) and rods (1.0 μm) dominate in the meso-trophic CS, and we argue that this could be due to the allochthonous input of more recalcitrant organic matter.

4.2. Microbial Functioning: Production and Decomposition Processes

Organic Carbon produced by PP is taken up by bacteria to support their growth and metabolism [74,75]; in addition, through PHP, prokaryotes are able to uptake and incorporate simple molecules released by enzyme hydrolysis of organic polymers. In the Gulf area, PP is highest in CS, where it falls in the range of meso-trophy, significantly supported by the micro-fraction as it generally happens in highly trophic environments [2]. The reduction of photosynthetic activity in IS and OS is accompanied by relative changes in the size-fraction contribution: the micro-fraction is replaced by the pico-fraction while the nano-fraction is halved.

PP rates data in the Southern Adriatic are scarce and mostly derived from distribution models or annual approximations on a basin scale [76]; winter values measured close to the Gulf range from 1 to 5 mgC m⁻³ h⁻¹ [77]. These values are comparable with the spring ones measured in the southern part of the Gulf where the nano-sized fraction (<10 µm) predominates. Observing the annual cycle of phytoplankton, some authors measured spring peaks that agree with our data [57,63] as well as the PP rates modelled for the entire Adriatic basin [78].

Microbial enzyme patterns and activity rates do not show significant variations in relation to the trophic status, caused by shifts in the dominant species or in enzyme expression by the same species in response to available organic substrates [79–82]. Decreasing enzyme levels from meso-CS towards oligo-trophic OS are commonly found in the Adriatic Sea [83,84] and the Ionian Sea [58,85–87]. In particular, high AP rates measured in CS compared to OS indicate a quick remineralization of organic Phosphorus, with release of inorganic Phosphorus sustaining high trophism (Figure 7). The high proteolytic activity (LAP) detected in IS and OS with respect to CS is consistent with the biopolymeric Carbon accumulation in the inner part of the Gulf [21]. Finally, higher a- and b-GLU rates in CS than in OS reflect the ability of the microbial community to metabolize the available polysaccharides, releasing glucose and cellobiose from the hydrolysis of starch and disaccharides, respectively. Our enzymatic data are similar to those measured in the Central Ionian Sea in autumn [88], although about one order of magnitude higher than those measured in the Ionian basin [89] and in the Strait of Otranto [7] in the same seasonal period of this study. In addition, the vertical decreasing enzyme profiles are in agreement with previous observations from the Ionian Sea [58,85,88,89] as well as from the Southern Adriatic Sea [7].

Similar to the enzyme activities, PHP follows a decreasing trend from CS to OS, where a minimum rate, about one tenth compared to CS, is reached. A similar spatial distribution of productive processes, decreasing with depth, was observed in the Southern Adriatic Sea [7].

4.3. Microbial Traits as Descriptors of Ecological Quality

A set of indices derived from the measured autotrophic and heterotrophic standing stocks and processes define the microbial traits related to the trophic pathways of the Systems (CS, IS and OS) identified within the Gulf.

Indices related to the autotrophic microbial community and its size-fractions (AN, P/B ratio, C-fate, Gi) are suitable descriptors of the process of organic Carbon production and its fate, as well as of the trophic pathway and grazing pressure.

The Assimilation Number (AN) gives insights on the growth rate and photosynthetic efficiency of phytoplankton community (Figure 3). The lowest ANs detected in CS suggest the steady state of such community, compared to almost double values found in IS and OS, that indicate an active phytoplankton growth. Indeed, the size fraction analysis shows that in IS this greater photosynthetic efficiency is due to pico-sized fraction while in OS to both pico- and micro- ones; conversely, no significant differences are noticed between CS and OS regarding the nano-fraction.

Indications on the potential fate of the biogenic Carbon pool are provided by the P:B ratio [90], whose values suggest in CS the occurrence of a dynamic balance between production and export of Carbon mediated by the nano- and micro- sized fractions; here the micro-fraction is mostly responsible for the export of biogenic Carbon. A different scenario is observed in IS and OS, where P:B ratios suggest that the photosynthesized Carbon is preferentially recycled within the System (Figure S2).

Besides the export through sedimentation and advection processes, the fate of biogenic Carbon depends on the grazing pressure on micro- and nano-fractions, as indicated by the potential Grazing index (GI, [55]). Its value is higher in CS, where mesotrophic conditions exist, while no evident signals of grazing pressure are found in the other Systems (Figure S3).

All these findings lead to identify two different biogenic Carbon pathways (herbivorous and multivorous) in the Gulf of Manfredonia during spring [2,11,91]. In IS and OS the phytoplankton-related standing stocks and processes suggest the predominance of a common multivorous pathway. In CS, a clear tendency towards the herbivorous pathway is recognized.

In addition, indices related to the heterotrophic microbial component [PP/PHP, LAP/AP, LAP/b-GLU and (LAP + aGLU + b-GLU)/PHP] can be suitable descriptors of different ecosystem functioning.

In marine environments, the proportion of PP supporting PHP is about 30–40% [75,92]. In the Western Mediterranean Sea, Turley et al. [93] estimated that PHP accounted for a mean percentage of 21% of PP, ranging from 9 to 46%.

In the Gulf of Manfredonia, PP/PHP ratio, as an index of the relative balance between primary (autotrophic) and secondary (heterotrophic) processes, shows the lowest values in CS, suggesting that these processes are reciprocally balanced more in CS than in IS and OS. When plotting PP vs. PHP an overall significant positive linear relationship (slope = 6.84, $r = 0.302$, $n = 27$, $P < 0.05$) is found, suggesting an increase in PHP by about 7 times per every unit increase of PP. However, looking at each System, where PP/PHP ratios are lowest, a direct relationship is observed (CS and OS, 13.9 and 21.4, respectively) suggesting that PP is a source of DOC for PHP in these Systems [93]. Conversely, in IS, the inverse relationship indicates the uncoupling between autotrophic and heterotrophic processes, with a maximum PP/PHP ratio (32.4) implying an active photosynthetic production compared to the heterotrophic one.

LAP/AP molar ratio is an index that gives insights on the N/P ratio. It gradually increases moving from CS to IS and OS, suggesting that in OS Nitrogen is more actively recycled than Phosphorus and largely available to microbial metabolism, while low ratios found in CS reflect the availability of Phosphorus provided by AP to sustain phytoplankton growth. Since enzyme activity estimates provide an information on nutrient acquisition mediated by microbial hydrolysis [94] and the stoichiometry of enzyme activities is indicative of the relative nutrient limitations on microbial assemblages in aquatic ecosystems [95], the molecular ratios between the enzyme activities allow to determine the utilization rates of organic compounds and microbial nutrient demand; therefore, compared to nutrient concentration, this ratio links the information on the nutrient pools to the microbial metabolism.

An indication of the quality of the organic matter is provided by LAP/b-GLU ratio, as an index of the relative importance of the decomposition of proteins with respect to polysaccharides. In the study area, this ratio always exceeded 1.0, suggesting the labile nature of polymeric compounds [58,84]. In CS, the polysaccharidic material derived from PP is more abundant than in IS and OS, where proteins predominate.

Furthermore, the ratio between enzymatic hydrolysis and uptake of monomers for prokaryotic production [(LAP + a-GLU + b-GLU)/PHP] indicates the amount of the monomers released by enzyme decomposition that is incorporated into PHP; its values in-

crease from CS (5.0) towards OS (74.1), suggesting in CS an efficient heterotrophic production compared to OS, where the monomers are released in amounts greater than those used for PHP.

4.4. Overall Late Spring Microbial Functioning in the Gulf Area

In synthesis, in spite of a low phytoplankton growth rate and photosynthetic efficiency, CS hosts in its meso-trophic waters an active herbivorous food chain able to export the produced biogenic Carbon, about 50% of which is available to grazers. In this System, micro-sized diatoms and dinoflagellates dominate and phytoplankton succession proceeds towards the second stage favored by low turbulence [70,96]. An active metabolism, mostly of organic phosphates and polysaccharides, allows the regeneration of the pool of nutrients. The released monomers are efficiently incorporated into new prokaryotic biomass (PHP). Correlations provide evidence that LAP, a- and b-GLU synthesis is stimulated by PP; AP is produced by total phytoplankton mostly with coccolithophorids ($r = 0.75$, $p < 0.05$) and is particularly active in the low salinity waters ($r = -0.73$, $p < 0.05$). The good coupling between auto- and heterotrophic productive processes is suggested by significant relationships linking total, pico- and micro- sized *chl a* with PHP ($r = 0.76$, 0.78 and 0.63 , $p < 0.05$, respectively).

An opposite scenario is observed in OS, where oligo-trophic waters host a phytoplankton community characterized by high growth rate and photosynthetic efficiency mostly in the pico-sized fraction, resulting in a limited export of the produced biogenic Carbon through advection and mesoscale circulation patterns. A “young” phytoplankton eukaryotic community including nano-sized diatoms and dinoflagellates exploits very efficiently nutrients by adopting an r-strategy (first stage of the succession *sensu* Margalef [70]). Temperature affects negatively both auto- and hetero-trophic microbial communities, as indicated by its negative relationships with total and micro-sized PP ($r = -0.55$ and -0.49 , $p < 0.05$, respectively) and total and micro-sized phytoplankton biomass as *chl a* ($r = -0.52$ and -0.63 , $p < 0.05$, respectively), as well as with PPA and PPT ($r = -0.55$ and -0.47 , $p < 0.05$, respectively). In OS, a strong reduction in the pool of nutrients is observed, as well as a low capability of the microbial assemblage to convert the mobilized Carbon and Phosphorus into prokaryotic biomass, resulting in a lower pool of monomers but still characterized by a good nutritional quality in terms of protein content as indicated by high LAP activity rates. AP is related to total phytoplankton and mostly to dinoflagellates ($r = 0.49$, $p < 0.05$), as well as to PP with its micro- and nano-fractions ($r = 0.59$, 0.60 , $p < 0.05$, respectively).

Between the two extreme conditions of CS and OS, there is IS, where nano- and pico-sized phytoplankton sustain a condition of equilibrium between the herbivorous and multivorous trophic pathways; therefore, this system is similar to OS with higher trophic conditions due to its close proximity to CS as well as to inputs from the mesoscale circulation entering from the Northern Adriatic basin. In these “complementary” waters, a high number of eukaryotic phytoplankton species find resources for their growth. Here microbial metabolism is sustained by the decomposition of organic phosphates and proteins, as suggested by the inverse correlations relating total PP and its micro- and pico-sized fractions with AP ($r = -0.67$, -0.74 , $p < 0.05$, -0.45 , $p < 0.05$, respectively) and LAP ($r = -0.57$, $p < 0.05$, -0.43 , -0.51 , $p < 0.05$, respectively). Conversely, the synthesis of b-GLU, able to decompose polysaccharides, is still stimulated by PP ($r = 0.47$, 0.43 , 0.52 , $p < 0.05$, with total, micro- and nano-sized PP, respectively). The Table S7 resumes the quality indicators of each System.

Even if the presented data refer to a single condition, they allowed us to build a conceptual model that represents the functioning of the observed Systems in the late spring period and could be exported to other coastal ecosystems. According to these findings, the Gulf of Manfredonia exhibited a clear distinction among the Coastal, Intermediate and Offshore Systems mainly based on their haline and depth characteristics.

In the light of the above-reported considerations and in compliance with the ultimate goal of our study, an attempt has been made to describe the ecological status of the Gulf area. According to the previous studies that used microbial parameters to assess the ecological quality of aquatic ecosystems [97–100], a qualitative judgment can be assigned to each System according to a multiple set of variables that takes into account the structure of the community (i.e., species and size composition) and its activities (i.e., production/decomposition processes), as reported below:

CS: environment rich in PPT and PPA abundances, characterized by quick organic matter recycling and good organic matter quality, exhibiting well-balanced PP and PHP processes, with the herbivorous pathway able to sustain high Gi pressure. In this System, a good Organic Matter transfer capability towards the upper trophic levels is found (HIGH);

OS: environment with low PPT and PPA abundances, still high organic matter quality in spite of low enzyme activity and PHP, low recycled PP sustained by pico- and nano-sized fractions without Gi pressure (GOOD);

IS: environment with intermediate PPT and PPA abundances, characterized by moderate enzyme activity rates, with a good organic matter quality and low PP and PHP (MODERATE);

DS: a reference environment (due to the limited number of samples) characterized by scarce microbial metabolism, low enzyme activity rates and PHP, allowing an active organic matter turnover; no anoxic conditions are observed (SUFFICIENT).

A further degree of system quality, although not identified in this study, could be included in this tentative judgment scale: environment with high organic matter production not associated to prompt recycling, anoxic/eutrophication phenomena or toxic algal blooms, low organic matter export towards upper trophic levels (BAD).

Supplementary Materials: The following are available online at www.mdpi.com/2073-4441/13/9/1325/s1. Figure S1: Output of the multivariate analyses: (a) Canonical Variates Analysis (CVA), (b) Canonical Correspondence Analysis (CCA). Figure S2: Scatter plots of the Production/Biomass ratio for micro- and nano-phytoplankton ($P/B [(PL/PT)/(BL/BT)]$) and for pico-phytoplankton ($P/B [(Ps/PT)/(Bs/BT)]$) in the Gulf Systems (CS, IS and OS). The fate of the biogenic Carbon pool through export-from or recycling-in the System was analyzed as described by Tremblay and Legendre [90]. Figure S3: Grazing index (Gi) calculated as $phaeo/(phaeo + chl a)$. (a) Boxplot of Gi of the micro- and nano-phytoplankton fractions in the Systems (CS, IS and OS). (b) The scatter diagrams of Gi vs. BL% of the two Systems (CS and IS) give indications about the grazing activities on micro- and nano-phytoplankton fractions, and a negative linear relationship, when BL > 50%, confirms its potential effect on the grazed pool [55]. Table S1: Sampling date and time, geographical coordinates, characteristics of the stations and assignment to the four identified clusters (CS: Coastal System, IS: Intermediate System, OS: Offshore System and DS: Deep System). Table S2: Parameter acronyms used in the text. Table S3: Main waters and biotic parameters measured in the four identified clusters (CS: Coastal System, IS: Intermediate System, OS: Offshore System and DS: Deep System) and in the Gulf area. Table S4: Total and size-fractionated prokaryotic and phytoplankton abundances measured in the four identified clusters (CS: Coastal System, IS: Intermediate System, OS: Offshore System and DS: Deep System) and in the Gulf area. Table S5: List of autotrophic phytoplankton taxa identified in the Gulf of Manfredonia during the study period. Table S6: Main Microbial activities measured in the four identified clusters (CS: Coastal System, IS: Intermediate System, OS: Offshore System and DS: Deep System) and in the Gulf. Table S7: Phytoplankton phase *sensu* Margalef [70] *; ratios between the analyzed parameters; main trophic pathways Herbivorous (H), Multivorous (M), Microbial loop (Mi); and Ecological Status.

Author Contributions: Conceptualization, F.D. and A.B.; methodology, all the authors.; software, A.B.; validation, all the authors; formal analysis, A.B.; investigation, F.D., C.C., and G.C.; resources, F.D.; data curation, all the authors.; writing—original draft preparation, all the authors; writing—review and editing, all the authors; visualization, A.B.; supervision, F.D. All authors have read and agreed to the published version of the manuscript.

Funding: This study is based on original data collected during the Programme Cluster10-SAM (2000–2005) and elaborated within the Project Sustainable Fishery DSS (2011–2016) both funded by the Italian Ministry of Research.

Institutional Review Board Statement: Not applicable.

Informed Consent Statement: Not applicable.

Data Availability Statement: Data are contained within the article and Supplementary Materials.

Conflicts of Interest: The authors declare no conflicts of interest.

References

1. Liu, J.; Meng, Z.; Liu, X.; Zhang, X.-H. Microbial assembly, interaction, functioning, activity and diversification: A review derived from community compositional data. *Mar. Life Sci. Technol.* **2019**, *1*, 112–128, doi:10.1007/s42995-019-00004-3.
2. Cermeño, P.; Maraño, E.; Pérez, V.; Serret, P.; Fernandez, E.; Castr, C.G. Phytoplankton size structure and primary production in a highly dynamical coastal ecosystem (Ría de Vigo, NW-Spain): Seasonal and short-time scale variability. *Estuar. Coast. Shelf Sci.* **2006**, *67*, 251–266, doi:10.1016/j.ecss.2005.11.027.
3. D’Alelio, D.; Libralato, S.; Wyatt, T.; Ribera d’Alcalà, M. Ecological-network models link diversity, structure and function in the plankton food-web. *Sci. Rep.* **2016**, *6*, 21806, doi:10.1038/srep21806.
4. Ducklow, H. Bacterial production and biomass in the oceans. In *Microbial Ecology of the Oceans*; Kirchman, D.L., Ed.; Wiley-Liss, Inc.: Wilmington, NC, USA, 2000; pp. 85–120.
5. Sarmiento, H.; Montoya, J.M.; Vázquez-Domínguez, E.; Vaqué, D.; Gasol, J.M. Warming effects on marine microbial food web processes: How far can we go when it comes to predictions? *Philos. Trans. R. Soc. Lond. B Biol. Sci.* **2010**, *12*, 2137–2149, doi:10.1098/rstb.2010.0045.
6. La Ferla, R.; Leonardi, M. Ecological implications of biomass and morphotype variations of bacterioplankton: An example in a coastal zone of the Northern Adriatic Sea (Mediterranean). *Mar. Ecol.* **2005**, *26*, 82–88, doi:10.1111/j.1439-0485.2005.00049.x.
7. Azzaro, M.; La Ferla, R.; Maimone, G.; Monticelli, L.S.; Zacccone, R.; Civitarese, G. Prokaryotic dynamics and heterotrophic metabolism in a deep-convection site of Eastern Mediterranean Sea (the Southern Adriatic Pit). *Cont. Shelf Res.* **2012**, *44*, 106–118, doi:10.1016/j.csr.2011.07.011.
8. Gasol, J.M.; del Giorgio, P.A.; Massana, R.; Duarte, C.M. Active versus inactive bacteria: Size-dependence in a coastal marine plankton community. *Mar. Ecol. Prog. Ser.* **1995**, *128*, 91–97, doi:10.3354/meps128091.
9. Cotner, J.; Biddanda, B. Small players, large role: Microbial influence on biogeochemical processes in pelagic aquatic ecosystems. *Ecosystems* **2002**, *5*, 105–121, doi:10.1007/s10021-001-0059-3.
10. Legendre, L.; Rassoulzadegan, F. Plankton and nutrient dynamics in marine waters. *Ophelia* **1995**, *41*, 153–172, doi:10.1080/00785236.1995.10422042.
11. Legendre, L.; Rassoulzadegan, F. Food-web mediated export of biogenic carbon in oceans: Environmental control. *Mar. Ecol. Prog. Ser.* **1996**, *145*, 179–193, doi:10.3354/meps145179.
12. Van Wambeke, F.; Heussner, S.; Diaz, F.; Raimbault, P.; Conan, P. Small-scale variability in the coupling/uncoupling of bacteria, phytoplankton and organic carbon fluxes along the continental margin of the Gulf of Lyons, Northwestern Mediterranean Sea. *J. Mar. Syst.* **2002**, *33–34*, 411–429, doi:10.1016/S0924-7963(02)00069-6.
13. Christaki, U.; Van Wambeke, F.; Lefevre, D.; Lagaria, A.; Prieur, L.; Pujó-Pay, M.; Grattepanche, J.-D.; Colombet, J.; Psarra, S.; Dolan, J.R.; et al. Microbial food webs and metabolic state across oligotrophic waters of the Mediterranean Sea during summer. *Biogeosciences* **2011**, *8*, 1839–1852, doi:10.5194/bg-8-1839-2011.
14. Zacccone, R.; Azzaro, M.; Azzaro, F.; Caruso, G.; Caroppo, C.; Decembrini, F.; Diociaiuti, T.; Fonda Umani, S.; Leonardi, M.; Maimone, G.; et al. Trophic structure and microbial activity in a spawning area of *Engraulis encrasicolus*. *Estuar. Coast. Shelf Sci.* **2018**, *207*, 215–222, doi:10.1016/j.ecss.2018.04.008.
15. Siokou-Frangou, I.; Christaki, U.; Mazzocchi, M.G.; Montresor, M.; Ribera d’Alcalá, M.; Vaqué, D.; Zingone, A. Plankton in the open Mediterranean Sea: A review. *Biogeosciences* **2010**, *7*, 1543–1586, doi:10.5194/bg-7-1543-2010.
16. Varkitzi, I.; Francé, J.; Basset, A.; Cozzoli, F.; Stanca, E.; Zervoudaki, S.; Giannakourou, A.; Assimakopoulou, G.; Venetsanopoulou, A.; Mozetič, P.; et al. Pelagic habitats in the Mediterranean Sea: A review of Good Environmental Status (GES) determination for plankton components and identification of gaps and priority needs to improve coherence for the MSFD implementation. *Ecol. Indic.* **2018**, *95*, 203–218, doi:10.1016/j.ecolind.2018.07.036.
17. Zoccarato, L.; Malusà, A.; Fonda Umani, S. Major contribution of prokaryotes to carbon fluxes in the pelagic microbial food webs of the Mediterranean Sea. *Adv. Oceanogr. Limnol.* **2016**, *7*, 51–66, doi:10.4081/aiol.2016.5799.
18. Bianchi, C.N.; Zurlini, G. Criteri e prospettive di una classificazione ecotipologica dei sistemi marini costieri italiani. *Acqua Aria* **1984**, *8*, 785–796.
19. Spagnoli, F.; Bartholini, G.; Dinelli, E.; Giordano, P. Geochemistry and particle size of surface sediments of gulf of Manfredonia (southern Adriatic Sea). *Estuar. Coast. Shelf Sci.* **2008**, *80*, 21–30, doi:10.1016/j.ecss.2008.07.008.

20. Spagnoli, F.; Dell'Anno, A.; de Marco, A.; Dinelli, E.; Fabiano, M.; Gadaleta, M.V.; Ianni, C.; Loiacono, F.; Manini, E.; Marini, M.; et al. Biogeochemistry, grain size and mineralogy of the central and southern Adriatic sea sediments: A review. *Chem. Ecol.* **2010**, *26*, 19–44, doi:10.1080/02757541003689829.
21. Fossile, E.; Sabbatini, A.; Spagnoli, F.; Caridi, F.; Dell'Anno, A.; de Marco, R.; Dinelli, E.; Droghini, E.; Tramontana, M.; Negri, A. Sensitivity of foraminiferal-based indices to evaluate the ecological quality status of marine coastal benthic systems: A case study of the Gulf of Manfredonia (southern Adriatic Sea). *Mar. Pollut. Bull.* **2021**, *163*, 111933, doi:10.1016/j.marpolbul.2020.111933.
22. Cattaneo, A.; Correggiari, A.; Langone, L.; Trincardi, F. The late-Holocene Gargano subaqueous delta, Adriatic shelf: Sediment pathways and supply fluctuations. *Mar. Geol.* **2003**, *193*, 61–91, doi:10.1016/S0025-3227(02)00614-X.
23. Artigiani, A.; Paschini, E.; Russo, A.; Bregant, D.; Raicich, F.; Pinardi, N. The Adriatic Sea general circulation: Part II: Baroclinic circulation structure. *J. Phys. Oceanogr.* **1997**, *27*, 1515–1532, doi:10.1175/1520-0485(1997)027<1492:TASGCP>2.0.
24. Manca, B.B.; Kovačević, V.; Gačić, M.; Viezzoli, D. Dense water formation in the Southern Adriatic Sea and spreading into the Ionian Sea in the period 1997–1999. *J. Mar. Syst.* **2002**, *33–34*, 133–154, doi:10.1016/S0924-7963(02)00056-8.
25. Sellschopp, J.; Álvarez, A., Dense low-salinity out-flow from the Adriatic Sea under mild (2001) and strong (1999) winter conditions. *J. Geophys. Res.* **2003**, *108*, 8104, doi:10.1029/2002JC001562.
26. Sciascia, R.; Berta, M.; Carlson, D.F.; Griffa, A.; Panfili, M.; La Mesa, M.; Corgnati, L.; Mantovani, C.; Domenella, E.; Fredj, E.; et al. Linking sardine recruitment in coastal areas to ocean currents using surface drifters and HF radar: A case study in the Gulf of Manfredonia, Adriatic Sea. *Ocean Sci.* **2018**, *14*, 1461–1482, doi:10.5194/os-14-1461-2018.
27. Guglielmo, R.; Bergamasco, A.; Minutoli, R.; Patti, F.P.; Belmonte, G.; Spanò, N.; Zagami, G.; Bonanzinga, V.; Guglielmo, L.; Granata, A. The Otranto Channel (South Adriatic Sea), a hot-spot area of plankton biodiversity: Pelagic polychaetes. *Sci. Rep.* **2019**, *9*, 19490, doi:10.1038/s41598-019-55946-6.
28. Aminot, A.; Chausseped, M. *Manuel des Analyses Chimiques en Milieu Marin*, Jouve ed.; Centre National pour l'Exploitation des Océans: Brest, France, 1983; pp. 1–395.
29. Strickland, J.D.H.; Parsons, T.R. *A Practical Hand Book of Seawater Analysis*, 2nd ed.; Fisheries Research Board of Canada Bulletin 157: Ottawa, ON, Canada, 1972; pp. 1–310.
30. Decembrini, F.; Hopkins, T.S.; Azzaro, F. Variability and sustenance of the deep-chlorophyll maximum over a narrow shelf, Augusta gulf (Sicily). *Chem. Ecol.* **2004**, *20*, S231–S247, doi:10.1080/02757540410001699677.
31. Lorenzen, C.I. Determination of chlorophyll and phaeopigments spectro-photometric equations. *Limnol. Oceanogr.* **1967**, *12*, 343–346.
32. Santos, M.; Mouriño, H.; Moita, M.T.; Silva, A.; Amorim, A.; Oliveira, P.B. Characterizing phytoplankton biomass seasonal cycles in two NE Atlantic coastal bays. *Cont. Shelf Res.* **2020**, *207*, 104200, doi:10.1016/j.csr.2020.104200.
33. Steeman-Nielsen, E. The use of radioactive carbon (¹⁴C) for measuring organic production in the sea. *J. Cons. Int. Explor. Mer* **1952**, *18*, 117–140.
34. Decembrini, F.; Bergamasco, A.; Mangoni, O. Seasonal characteristics of size-fractionated phytoplankton community and fate of photosynthesized carbon in a sub-Antarctic area (Straits of Magellan). *J. Mar. Syst.* **2014**, *136*, 31–41, doi:10.1016/j.jmarsys.2014.03.008.
35. Porter, K.G.; Feig, Y.S. The use of DAPI for identifying and counting aquatic microflora. *Limnol. Oceanogr.* **1980**, *25*, 943–948.
36. Massana, R.; Gasol, J.P.; Björnson, P.K.; Blackburn, N.; Hanström, A.; Hietanen, S.; Hygum, B.H.; Kuparinen, J.; Pedros-Aliò, C. Measurement of bacterial size via image analysis of epifluorescence preparations: Description of an inexpensive system and solutions to some of the most common problems. *Sci. Mar.* **1997**, *6*, 397–407.
37. Bratbak, G. Bacterial biovolume and biomass estimation. *Appl. Environ. Microbiol.* **1985**, *49*, 1488–1493.
38. Edler, L.; Elbrächter, M. The Utermöhl method for quantitative phytoplankton analysis. In *Microscopic and Molecular Methods for Quantitative Phytoplankton Analysis*; Karlson, B., Cusack, C., Bresnan, E., Eds.; UNESCO IOC Manuals and Guides n. 55: Paris, France, 2010; pp. 13–20.
39. Tomas, C. *Identifying Marine Phytoplankton*; Academic Press: San Diego, CA, USA, 1997; p. 858.
40. Hoppe, H.G. Phosphatase activity in the sea. *Hydrobiologia* **2003**, *493*, 187–200, doi:10.1023/A:1025453918247.
41. Caruso, G. Leucine aminopeptidase, β -glucosidase and alkaline phosphatase activity rates and their significance in nutrient cycles in some coastal Mediterranean sites. *Mar. Drugs* **2010**, *8*, 916–940, doi:10.3390/md8040916.
42. Monticelli, L.S.; Caruso, G.; Decembrini, F.; Caroppo, C.; Fiesoletti, F. Role of prokaryotic biomasses and activities in Carbon and Phosphorus cycles at a coastal, thermohaline front and in offshore waters (Gulf of Manfredonia, Southern Adriatic Sea). *Microb. Ecol.* **2014**, *67*, 501–519, doi:10.1007/s00248-013-0350-9.
43. Smith, D.C.; Azam, F. A simple, economical method for measuring bacterial protein synthesis rates in seawater using ³H-leucine. *Mar. Microb. Food Webs* **1992**, *6*, 107–114.
44. Kirchman, D.L. Leucine incorporation as a measure of biomass production by heterotrophic bacteria. In *Handbook of Methods in Aquatic Microbial Ecology*; Kemp, P.F., Sherr, B.F., Sherr, E.B., Eds.; Lewis Publisher: Boca Raton, FL, USA, 1993; pp. 509–512.
45. Pollard, P.C.; Moriarty, D.J.W. Validity of the tritiated thymidine methods for estimating bacterial growth rates: Measurement of isotope dilution during DNA synthesis. *Appl. Environ. Microbiol.* **1984**, *48*, 1076–1083.
46. Schlitzer, R. Ocean Data View. 2001. Available online: <https://odv.awi.de/software/download/> (accessed on 26 March 2021).
47. Strauss, T.; von Maltitz, M.J. Generalising Ward's Method for Use with Manhattan Distances. *PLoS ONE* **2017**, *12*, e0168288, <https://doi.org/10.1371/journal.pone.0168288>.

48. Venables, W.N.; Ripley, B.D. *Modern Applied Statistics with S*, 4th ed.; Springer: New York, NY, USA, 2002; pp. 1–495, ISBN 0-387-95457-0.
49. Clarke, K.R.; Gorley, R.N.; Somerfield, P.J., Warwick, R.M. *Change in Marine Communities: An Approach to Statistical Analysis and Interpretation*, 3rd ed.; PRIMER-E Ltd: Plymouth, UK, 2014.
50. Clarke, K.R.; Tweedly, J.R.; Valesini, F.J. Simple shade plots aid better long-term choices of data pre-treatment in multivariate assemblage studies. *J. Mar. Biol. Assoc. U. K.* **2014**, *94*, 1–16, doi:10.1017/S0025315413001227.
51. Clarke, K.R. Non-parametric multivariate analyses of changes in community structure. *Aust. J. Ecol.* **1993**, *18*, 117–143, doi:10.1111/j.1442-9993.1993.tb00438.x.
52. Legendre, P.; Legendre, L. *Numerical Ecology*, 2nd ed.; Elsevier Science: Amsterdam, The Netherlands, 1998; pp. 1–853, ISBN 9780080537870.
53. Hammer, Ø.; Harper, D.A.T.; Ryan, P.D. PAST: Paleontological statistics software package for education and data analysis. *Palaeontol. Electron.* **2001**, *4*, 1–9.
54. Yacobi, Y.Z.; Zohary, T. Carbon: Chlorophyll a ratio, assimilation numbers and turnover times of Lake Kinneret phytoplankton. *Hydrobiologia* **2010**, *639*, 185–196, doi:10.1007/s10750-009-023-3.
55. Tamigneaux, E.; Legendre, L.; Klein, B.; Mingelbier, M. Seasonal dynamics and potential fate of size-fractionated phytoplankton in a temperate nearshore environment (Western Gulf of St. Lawrence, Canada). *Estuar. Coast. Shelf Sci.* **1999**, *48*, 253–269, doi:10.1006/ecss.1999.0416.
56. Totti, C.; Cangini, M.; Ferrari, C.; Kraus, R.; Pompei, M.; Pugnetti, A.; Romagnoli, T.; Vanucci, S.; Socal, G. Phytoplankton size-distribution and community structure in relation to mucilage occurrence in the northern Adriatic Sea. *Sci. Total Environ.* **2005**, *353*, 204–217, doi:10.1016/j.scitotenv.2005.09.028.
57. Cerino, F.; Bernardi Aubry, F.; Coppola, J.; La Ferla, R.; Maimone, G.; Socal, G.; Totti, C. Spatial and temporal variability of pico-, nano- and microphytoplankton in the offshore waters of the southern Adriatic Sea (Mediterranean Sea). *Cont. Shelf Res.* **2012**, *44*, 94–105, doi:10.1016/j.csr.2011.06.006.
58. Zaccone, R.; Caroppo, C.; La Ferla, R.; Zampino, D.; Caruso, G.; Leonardi, M.; Maimone, G.; Azzaro, M.; Sitran, R. Deep-Chlorophyll Maximum time series in the Augusta Gulf (Ionian Sea): Microbial community structures and functions. *Chem. Ecol.* **2004**, *20*, 267–284, doi:10.1080/02757540410001689812.
59. Caroppo, C.; Musco, L.; Stabili, L. Planktonic assemblages in a coastal Mediterranean area subjected to anthropogenic pressure. *J. Geogr. Nat. Disaster Biodiv. Conserv.* **2014**, *4*, 121, doi:10.4172/2167-0587.1000121.
60. Caroppo, C. Ecology and biodiversity of picoplanktonic cyanobacteria in coastal and brackish environments. *Biodivers. Conserv.* **2015**, *24*, 949–971, doi:10.1007/s10531-015-0891-y.
61. Specchiulli, A.; Bignami, F.; Marini, M.; Fabbrocini, A.; Scirocco, T.; Campanelli, A.; Penna, P.; Santucci, A.; D'Adamo, R. The role of forcing agents on biogeochemical variability along the southwestern Adriatic coast: The Gulf of Manfredonia case study. *Estuar. Coast. Shelf Sci.* **2016**, *183*, 136–149, doi:10.1016/j.ecss.2016.10.033.
62. Totti, C.; Romagnoli, T.; Accoroni, S.; Coluccelli, A.; Pellegrini, M.; Campanelli, A.; Grilli, F.; Marini, M. Phytoplankton communities in the northwestern Adriatic Sea: Interdecadal variability over a 30-years period (1988–2016) and relationships with meteorological drivers. *J. Mar. Syst.* **2019**, *193*, 137–153, doi:10.1016/j.jmarsys.2019.01.007.
63. Totti, C.; Civitarese, G.; Acri, F.; Barletta, D.; Candelari, G.; Paschini, E.; Solazzi, A. Seasonal variability of phytoplankton populations in the middle Adriatic sub-basin. *J. Plankton Res.* **2000**, *22*, 1735–1756, doi:10.1093/plankt/22.9.1735.
64. Caroppo, C.; Fiocca, A.; Sammarco, P.; Magazzù, G. Seasonal variations of nutrients and phytoplankton in the coastal SW Adriatic Sea (1995–1997). *Bot. Mar.* **1999**, *42*, 389–400, doi:10.1515/BOT.1999.045.
65. Socal, G.; Boldrin, A.; Bianchi, F.; Civitarese, G.; De Lazzari, A.; Rabitti, S.; Totti, C.; Turchetto, M.M. Nutrient, particulate matter and phytoplankton variability in the photic layer of the Otranto Strait. *J. Mar. Syst.* **1999**, *20*, 381–398, doi:10.1016/S0924-7963(98)00075.
66. Stabili, L.; Caroppo, C.; Cavallo, R.A. Monitoring of a coastal Mediterranean area: Culturable bacteria, phytoplankton, environmental factors and their relationships in the southern Adriatic Sea. *Environ. Monit. Assess.* **2006**, *121*, 303–325, doi:10.1007/s10661-005-9124-2.
67. Campanelli, A.; Cabrini, M.; Grilli, F.; Fornasaro, D.; Penna, P.; Kljajić, Z.; Marini, M. Physical, biochemical and biological characterization of two opposite areas in the Southern Adriatic Sea (Mediterranean Sea). *Open J. Mar. Sci.* **2013**, *3*, 120–130, doi:10.4236/ojms.2013.32013.
68. Caroppo, C.; Turicchia, S.; Margheri, M.C. Phytoplankton assemblages in coastal waters of the Northern Ionian Sea (eastern Mediterranean), with special reference to cyanobacteria. *J. Mar. Biol. Assoc. U. K.* **2006**, *86*, 927–937, doi:10.1017/S0025315406013889.
69. Decembrini, F.; Caroppo, C.; Bergamasco, A. Influence of lateral advection on phytoplankton size-structure and composition in a Mediterranean coastal area. *Cont. Shelf Res.* **2020**, *209*, 104216, doi:10.1016/j.csr.2020.104216.
70. Margalef, R. The food web in the pelagic environment. *Helgol. Wiss. Meer.* **1967**, *15*, 548–559.
71. Karuza, A.; Caroppo, C.; Camatti, E.; Di Poi, E.; Monti, M.; Stabili, L.; Auriemma, R.; Pansera, M.; Cibic, T.; Del Negro, P. 'End to end' planktonic trophic web and its implications for the mussel farms in the Mar Piccolo of Taranto (Ionian Sea, Italy). *Environ. Sci. Pollut. Res.* **2016**, *23*, 12707–12724, doi:10.1007/s11356-015-5621-1.
72. Jacquet, S.; Lennon, J.F.; Marie, D.; Vaultot, D. Picoplankton population dynamics in coastal waters of the northwestern Mediterranean Sea. *Limnol. Oceanogr.* **1998**, *43*, 1916–1921, doi:10.4319/lo.1998.43.8.1916.

73. Unanue, M.; Ayo, B.; Azua, I.; Barcina, I.; Iriberry, J. Temporal variability of attached and free-living bacteria in coastal waters. *Microb. Ecol.* **1992**, *23*, 27–39, doi:10.1007/BF00165905.
74. Azam, F.; Smith, D.C.; Carlucci, A.F. Bacterial transformation and transport of organic matter in the Southern California Bight. *Prog. Oceanogr.* **1992**, *30*, 151–166.
75. Ducklow, H.W.; Carlson, C.A. Oceanic Bacterial Production. In *Advances in Microbial Ecology*; Marshall, K.C., Ed.; Springer: Boston, MA, USA, 1992; Volume 12, doi:10.1007/978-1-4684-7609-5_3.
76. Catalano, G.; Azzaro, M.; Bastianini, M.; Bellucci, L.G.; Bernardi Aubry, F.; Bianchi, F.; Burca, M.; Cantoni, C.; Caruso, G.; Casotti, R.; et al. The Carbon budget in the northern Adriatic Sea, a winter case study. *J. Geophys. Res. Biogeosci.* **2014**, *119*, 1399–1417, doi:10.1002/2013JG002559.
77. Faganeli, J.; Gačić, M.; Malej, A.; Smodlaka, N. Pelagic organic matter in the Adriatic Sea in relation to winter hydrographic conditions. *J. Plankton Res.* **1989**, *11*, 1129–1141.
78. Zavatarelli, M.; Baretta, J.W.; Baretta-Bekker, J.G.; Pinardi, N. The dynamics of the Adriatic Sea ecosystem. An idealized model study. *Deep-Sea Res. Part I* **2000**, *47*, 937–970, doi:10.1016/S0967-0637(99)00086-2.
79. La Ferla, R.; Azzaro, M.; Caruso, G.; Monticelli, L.S.; Maimone, G.; Zaccone, R.; Packard, T.T. Prokaryotic abundance and heterotrophic metabolism in the deep Mediterranean Sea. *Adv. Oceanogr. Limnol.* **2010**, *1*, 143–166, doi:10.1080/19475721.2010.483336.
80. Caruso, G.; Decembrini, F.; Caruso, R.; Zappalà, G.; Leonardi, M.; Bergamasco, A. Are microbial enzyme activities sensitive indicators of the trophic state of marine ecosystems? In *Pollution Monitoring*; Ortiz, A.C., Griffin, N.B., Eds.; NOVA Publishers: Hauppauge, NY, USA, 2011; pp. 195–2010.
81. Celussi, M.; Del Negro, P. Microbial degradation at a shallow coastal site: Long-term spectra and rates of exoenzymatic activities in the NE Adriatic Sea. *Estuar. Coast. Shelf Sci.* **2012**, *115*, 75–86, doi:10.1016/j.ecss.2012.02.002.
82. Manna, V.; De Vittor, C.; Giani, M.; Del Negro, P.; Celussi, M. Long-term patterns and drivers of microbial organic matter utilization in the northernmost basin of the Mediterranean Sea. *Mar. Environ. Res.* **2021**, *164*, 105245, doi:10.1016/j.marenvres.2020.105245.
83. Caruso, G.; Zaccone, R. Estimates of leucine aminopeptidase activity in different marine and brackish environments. *J. Appl. Microbiol.* **2000**, *89*, 951–959, doi:10.1046/j.1365-2672.2000.01198.x.
84. Zaccone, R.; Caruso, G. Microbial hydrolysis of polysaccharides and organic phosphates in the Northern Adriatic Sea. *Chem. Ecol.* **2002**, *18*, 85–94, doi:10.1080/02757540212691.
85. Zaccone, R.; Monticelli, L.S.; Seritti, A.; Santinelli, C.; Azzaro, M.; Boldrin, A.; La Ferla, R.; Ribera d'Alcalà, M. Bacterial processes in the intermediate and deep layers of the Ionian Sea in winter 1999: Vertical profiles and their relationship to the different water masses. *J. Geophys. Res. Oceans* **2003**, *108*, doi:10.1029/2002JC001625.
86. Zaccone, R.; Caruso, G.; Azzaro, M.; Azzaro, F.; Crisafi, E.; Decembrini, F.; et al. Prokaryotic activities and abundance in pelagic areas of the Ionian Sea. *Chem. Ecol.* **2010**, *26*, 169–197, doi:10.1080/02757541003772914.
87. Zaccone, R.; Caruso, G. Microbial enzymes in the Mediterranean Sea: Relationship with climate changes. *AIMS Microbiol.* **2019**, *5*, 251–271, doi:10.3934/microbiol.2019.3.251.
88. Placenti, F.; Azzaro, M.; Artale, V.; La Ferla, R.; Caruso, G.; Santinelli, C.; Maimone, G.; Monticelli, L.; Quinci, E.M.; Sprovieri, M. Biogeochemical patterns and microbial processes in the Eastern Mediterranean Deep Water of Ionian Sea. *Hydrobiologia* **2018**, *815*, 97–112, doi:10.1007/s10750-018-3554-7.
89. Zaccone, R.; Boldrin, A.; Caruso, G.; La Ferla, R.; Maimone, G.; Santinelli, C.; Turchetto, M. Enzymatic activities and prokaryotic abundance in relation to organic matter along a West-East Mediterranean transect (TRANSMED cruise). *Microb. Ecol.* **2012**, *64*, 54–66, doi:10.1007/s00248-012-0011-4.
90. Tremblay, J.E.; Legendre, L. A model for the size-fractionated biomass and production of marine phytoplankton. *Limnol. Oceanogr.* **1994**, *39*, 2004–2014, doi:10.4319/lo.1994.39.8.2004.
91. Mousseau, L.; Klein, B.; Legendre, L.; Dauchez, S.; Tamigneaux, E.; Tremblay, J.-E.; Grant Ingram, R. Assessing trophic pathways that dominate planktonic food webs: An approach based on simple ecological ratios. *J. Plankton Res.* **2001**, *23*, 765–777, doi:10.1093/plankt/23.8.765.
92. Cole, J.J.; Findlay, S.; Pace, M.L. Bacterial production in fresh and saltwater ecosystems: A cross-system overview. *Mar. Ecol. Prog. Ser.* **1988**, *43*, 1–10.
93. Turley, C.M.; Bianchi, M.; Christaki, U.; Conan, P.; Harris, J.R.W.; Psarra, S.; Ruddy, G.; Stutt, E.D.; Tselepides, A.; Van Wambeke, F. Relationship between primary producers and bacteria in an oligotrophic sea: The Mediterranean and biogeochemical implications. *Mar. Ecol. Prog. Ser.* **2000**, *193*, 11–18, doi:10.1007/s00248-012-0011-4.
94. Arnosti, C.; Bell, C.; Moorhead, D.L.; Sinsabaugh, R.L.; Steen, A.D.; Stromberger, M.; Wallenstein, M.; Weintraub, M.N. Extracellular enzymes in terrestrial, freshwater, and marine environments: Perspectives on system variability and common research needs. *Biogeochemistry* **2014**, *117*, 5–21, doi:10.1007/s10533-013-9906-5.
95. Hill, B.H.; Elonen, C.M.; Seifert, L.R.; May, A.A.; Tarquinio, E. Microbial enzyme stoichiometry and nutrient limitation in US streams and rivers. *Ecol. Indic.* **2012**, *18*, 540–551, doi:10.1016/j.ecolind.2012.01.007.
96. Wyatt, T. Margalef's mandala and phytoplankton bloom strategies. *Deep-Sea Res. Part II* **2014**, *101*, 32–49, doi:10.1016/j.dsr2.2012.12.006.

97. Mazzola, A.; Bergamasco, A.; Calvo, S.; Caruso, G.; Chemello, R.; Colombo, F.; Giaccone, G.; Gianguzza, P.; Guglielmo, L.; Leonardi, M.; et al. Sicilian transitional waters: Current status and future development. *Chem. Ecol.* **2010**, *26*, 267–283, doi:10.1080/02757541003627704.
98. Caruso, G.; La Ferla, R.; Azzaro, M.; Zoppini, A.; Marino, G.; Petochi, T.; Corinaldesi, C.; Leonardi, M.; Zaccone, R.; Fonda-Umani, S.; et al. Microbial assemblages for environmental quality assessment: Knowledge, gaps and usefulness in the EC Marine Strategy Framework Directive. *Crit. Rev. Microbiol.* **2016**, *42*, 883–904, doi:10.3109/1040841X.2015.1087380.
99. Caruso, G.; Azzaro, M.; Caroppo, C.; Decembrini, F.; Monticelli, L.S.; Leonardi, M.; Maimone, G.; Zaccone, R.; La Ferla, R. Microbial community and its potential as descriptor of environmental status. *ICES J. Mar. Sci.* **2016b**, *73*, 2174–2177, doi:10.1093/icesjms/fsw101.
100. Ferrera, I.; Reñé, A.; Funosas, D.; Camp, J.; Massana, R.; Gasol, J.M.; Garcés, E. Assessment of microbial plankton diversity as an ecological indicator in the NW Mediterranean coast. *Mar. Pollut. Bull.* **2020**, *160*, 111691, doi:10.1016/j.marpolbul.2020.111691.